Synthesis and Reactions of *cis*-Silyl(boryl)platinum(II) Complexes

Takashi Sagawa, Yasuaki Asano, and Fumiyuki Ozawa*

Department of Applied Chemistry, Graduate School of Engineering, Osaka City University, Sumiyoshi-ku, Osaka 558-8585, Japan

Received August 20, 2002

Four kinds of silyl(boryl)platinum(II) complexes, **2a**−**2d**, have been prepared by oxidative addition of silylboranes to platinum(0) complexes, in situ generated from $Pt(cod)_2$ and 2 molar quantity of tertiary phosphine ligands (L) in Et_2O: *cis*-$Pt(SiMe_2Ph)(BX_2)L_2$ (X_2 = −$OCMe_2$-CMe_2O− (pin), L = PMe_3 (**2a**), PMe_2Ph (**2b**), PEt_3 (**2c**); X_2 = −$NMeCH_2CH_2NMe$− (dmeda), L = PMe_3 (**2d**)). Complexes **2a**−**2c** undergo selective insertion of phenylacetylene into the Pt−B bond at room temperature in CD_2Cl_2, giving *cis*-Pt{C(Ph)═CH(Bpin)}$(SiMe_2Ph)L_2$ (L = PMe_3 (**3a**), PMe_2Ph (**3c**), PEt_3 (**3c**)), respectively, while **2d** is inactive toward insertion. The X-ray structure of **3b** has been determined. Kinetic study using **2a** indicates the mechanism involving prior dissociation of L, followed by insertion of phenylacetylene into the Pt−B bond. The insertion complexes **3a**−**3c** undergo C−Si reductive elimination to give (*Z*)-α-silyl-*β*-borylstyrene. The reactivity decreases in the order **3c** ≫ **3b** > **3a**.

Introduction

Catalytic addition of inter-element linkages[1] to unsaturated hydrocarbons has attracted a great deal of recent interest.[2] The addition of silicon−element bonds catalyzed by platinum-group metal complexes is among the central subjects of such reactions. We have been interested in the reaction chemistry of platinum complexes which are responsible for these catalyses.[3−5] Although the catalytic mechanisms are frequently described by a simple extension of the common organometallic chemistry, the key intermediates presumed in the catalyses are not the organometallic compounds with metal−carbon or metal−hydrogen bonds, but a novel class of complexes bearing the linkages between metals and heavy elements. Reflecting the characteristic nature of heavy elements, these complexes should be unique in chemical properties. From this point of view, we have already synthesized bis(silyl)-, silyl(stannyl)-, and alkyl(silyl)platinum(II) complexes and found rather unusual structures and reactivities.[3] In this paper we report the synthesis and reactions of silyl(boryl)platinum(II) complexes, which have been assumed as a key intermediate for catalytic silylborylation of alkynes and alkenes,[2,6] but have never been observed in reality.

Scheme 1 illustrates the generally accepted catalytic cycle for silylborylation of alkynes. The first step is the oxidative addition of silylborane to a low-valent metal species (step a). While the resulting silyl−boryl intermediate possibly undergoes alkyne insertion into either the M−Si or M−B bond, it has been considered that the insertion into the M−B bond preferably takes place (step b) and the subsequent C−Si reductive elimination

* Corresponding author. E-mail: ozawa@a-chem.eng.osaka-cu.ac.jp.

(1) Tamao, K. *J. Organomet. Chem.* **2000**, *611*, 3.

(2) (a) Beletskaya, I.; Moberg, C. *Chem. Rev.* **1999**, *99*, 3435. (b) Suginome, M.; Ito, Y. *Chem. Rev.* **2000**, *100*, 3221. (c) Han, L.-B.; Tanaka, M. *Chem. Commun.* **1999**, 395. (d) Kondo, T.; Mistudo, T. *Chem. Rev.* **2000**, *100*, 3205.

(3) (a) Ozawa, F. *J. Organomet. Chem.* **2000**, *611*, 332. (b) Ozawa, F.; Kamite, J. *Organometallics* **1998**, *17*, 5630. (c) Ozawa, F.; Sakamoto, Y.; Sagawa, T.; Tanaka, R.; Katayama, H. *Chem. Lett.* **1999**, 1307. (d) Ozawa, F.; Hikida, T. *Organometallics* **1996**, *15*, 4501. (e) Hikida, T.; Onitsuka, K.; Sonogashira, K.; Hayashi, T.; Ozawa, F. *Chem. Lett.* **1995**, 985. (f) Ozawa, F.; Sugawara, M.; Hayashi, T. *Organometallics* **1994**, *13*, 3237. (g) Ozawa, F.; Sugawara, M.; Hasebe, K.; Hayashi, T. *Inorg. Chim. Acta* **1999**, *296*, 19.

(4) Related studies have been reported by several research groups. B−B: (a) Lesley, G.; Nguyen, P.; Taylor, N. J.; Marder, T. B. *Organometallics* **1996**, *15*, 5137. (b) Iverson, C. N.; Smith, M. R., III. *Organometallics* **1996**, *15*, 5155. (c) Ishiyama, T.; Matsuda, N.; Murata, M.; Ozawa, F.; Suzuki, A.; Miyaura, N. *Organometallics* **1996**, *15*, 713. (d) Clegg, W.; Lawlor, F. J.; Lesley, G.; Marder, T. B.; Norman, N. C.; Orpen, A. G.; Quayle, M. J.; Rice, C. R.; Scott, A. J.; Souza, F. E. S. *J. Organomet. Chem.* **1998**, *550*, 183. Ge−Ge: (e) Mochida, K.; Wada, T.; Suzuki, K.; Hatanaka, W.; Nishiyama, Y.; Nanjo, M.; Sekine, A.; Ohashi, Y.; Sakamoto, M.; Yamamoto, A. *Bull. Chem. Soc. Jpn.* **2001**, *74*, 123. Sn−Sn, Si−Si: (f) Obora, Y.; Tsuji, Y.; Nishiyama, K.; Ebihara, M.; Kawamura, T. *J. Am. Chem. Soc.* **1996**, *118*, 10922. (g) Tsuji, Y.; Nishiyama, K.; Hori, S.; Ebihara, M.; Kawamura, T. *Organometallics* **1998**, *17*, 507. Te−Si, Te−Ge, Te−Sn: (h) Han, L.-B.; Shimada, S.; Tanaka, M. *J. Am. Chem. Soc.* **1997**, *119*, 8133.

(5) For theoretical treatment of catalytic processes, see: B−B: (a) Cui, Q.; Musaev, D. G.; Morokuma, K. *Organometallics* **1997**, *16*, 1355. (b) Sakaki, S.; Kikuno, K. *Inorg. Chem.* **1997**, *36*, 226. Si−Si: (c) Sakaki, S.; Mizoe, N.; Sugimoto, M. *Organometallics* **1998**, *17*, 2510. (d) Sakaki, S.; Ogawa, M.; Musashi, Y. *J. Organomet. Chem.* **1997**, *535*, 25. (e) Sakaki, S.; Ogawa, M.; Kinoshita, M. *J. Phys. Chem.* **1995**, *99*, 9933. (f) Sakaki, S.; Ogawa, M.; Musashi, Y.; Arai, T. *J. Am. Chem. Soc.* **1994**, *116*, 7258. (g) Bottoni, A.; Higueruelo, A. P.; Miscione, G. P. *J. Am. Chem. Soc.* **2002**, *124*, 5506. Si−Sn: (h) Hada, M.; Tanaka, Y.; Ito, M.; Murakami, M.; Amii, H.; Ito, Y.; Nakatsuji, H. *J. Am. Chem. Soc.* **1994**, *116*, 8754. B−S: (i) Cui, Q.; Musaev, D. G.; Morokuma, K. *Organometallics* **1998**, *17*, 1383.

(6) (a) Suginome, M.; Nakamura, H.; Ito, Y. *Chem. Commun.* **1996**, 2777. (b) Onozawa, S.-y.; Hatanaka, Y.; Tanaka, M. *Chem. Commum.* **1997**, 1229. (c) Suginome, M.; Nakamura, H.; Ito, Y. *Angew. Chem., Int. Ed.* **1997**, *36*, 2516. (d) Suginome, M.; Matsuda, T.; Nakamura, H.; Ito, Y. *Tetrahedron* **1999**, *55*, 8787. (e) Suginome, M.; Nakamura, H.; Matsuda, T.; Ito, Y. *J. Am. Chem. Soc.* **1998**, *120*, 4248. (f) Suginome, M.; Matsuda, T.; Ito, Y. *Organometallics* **1998**, *17*, 5233. (g) Suginome, M.; Matsuda, T.; Yoshimoto, T.; Ito, Y. *Org. Lett.* **1999**, *1*, 1567. (h) Suginome, M.; Ohmori, Y.; Ito, Y. *Synlett* **1999**, *10*, 1567. (i) Onozawa, S.-y.; Hatanaka, Y.; Tanaka, M. *Chem. Commun.* **1999**, 1863. (j) Pohlman, T.; de Meijere, A. *Org. Lett.* **2000**, *2*, 3877. (k) Suginome, M.; Ohmori, Y.; Ito, Y. *J. Organomet. Chem.* **2000**, *611*, 403. (l) Suginome, M.; Matsuda, T.; Ito, Y. *J. Am. Chem. Soc.* **2000**, *122*, 11015. (m) Suginome, M.; Ohmori, Y.; Ito, Y. *J. Am. Chem. Soc.* **2001**, *123*, 4601. (n) Suginome, M.; Matsuda, T.; Yoshimoto, T.; Ito, Y. *Organometallics* **2002**, *21*, 1537.

10.1021/om020686z CCC: $22.00
Publication on Web 11/15/2002

Scheme 1

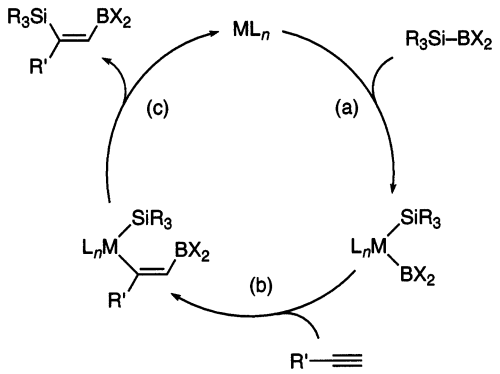

Scheme 2

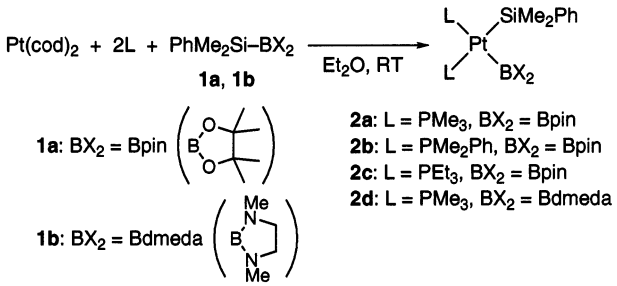

affords the silylborylation products (step c).[6] As described below, we have succeeded for the first time in observing all the elementary processes assumed in this scheme, using basic and compact tertiary phosphines as supporting ligands (L).

Results

Oxidative Addition of Silylboranes. Four kinds of silyl-boryl complexes, **2a**−**2d**, listed in Scheme 2 were prepared by the oxidative addition of silylboranes to Pt(cod)L_2 complexes, which were generated in situ from $Pt(cod)_2$ and 2 molar quantity of phosphines in Et_2O.[7] The pinacol derivative of silylborane **1a** rapidly reacted with PMe_3, PMe_2Ph, and PEt_3 complexes at room temperature to give **2a**−**2c**, quantitatively, as confirmed by $^{31}P\{^1H\}$ NMR spectroscopy. On the other hand, diaminosilylborane **1b** was much less reactive, and its reaction with $Pt(cod)(PMe_3)_2$ at room temperature took 12 h for completion.

The reaction of **1a** was examined further with other phosphine ligands ($PMePh_2$, PPh_3, PPr^i_3). In the case of $PMePh_2$, $^{31}P\{^1H\}$ NMR analysis of the reaction solution strongly suggested the formation of *cis*-Pt(SiMe$_2$Ph)(Bpin)($PMePh_2$)$_2$ (δ 11.8, $^1J_{PtP}$ = 1460 Hz), while its isolation was unsuccessful due to decomposition. The PPh_3 and PPr^i_3 complexes were totally unreactive even under heated conditions.

Complexes **2a**−**2d** were isolated as pale yellow solids and characterized by NMR spectroscopy and/or elemental analysis.[8] Figure 1a shows the $^{31}P\{^1H\}$ NMR spectrum of **2a**. Two sets of signals with ^{195}Pt satellites are observed. The sharp doublet at δ −17.4 with ^{29}Si satellites ($^2J_{SiP}$ = 148 Hz) is assignable to the phosphine trans to the silyl ligand, whereas the broad one at δ −19.0 arises from the phosphine trans to the boryl ligand. The broadening phenomenon observed in the latter signal is ascribed to the quadrupole coupling with ^{10}B and ^{11}B nuclei.

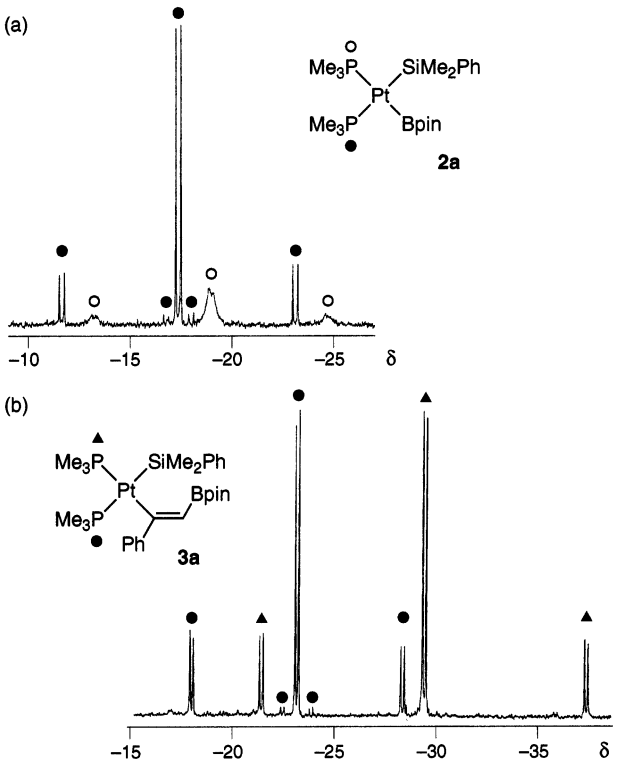

Figure 1. $^{31}P\{^1H\}$ NMR spectra of **2a** (a) and **3a** (b) in CD_2Cl_2.

Table 1. $^{31}P\{^1H\}$ NMR Data for 2a−2d in CD_2Cl_2 at −50 °C

complex	δ	assignment	$^1J_{PtP}$ (Hz)	$^2J_{SiP}$ (Hz)	$^2J_{PP}$ (Hz)
2a	−17.4 (d)	trans to Si	1374	148	29
	−19.0 (br)	trans to B	1375	0	
2b	−5.2 (br)	trans to B	1391	0	
	−6.4 (d)	trans to Si	1404	139	30
2c	+14.8 (br)	(overlap)[a]	1468	*b*	
2d	−12.6 (d)	trans to Si	1465	159	24
	−14.8 (br)	trans to B	1349	0	

[a] Two phosphorus atoms exhibited the same chemical shift. [b] Coupling constant was obscured due to broadening of the signal.

Table 1 lists the $^{31}P\{^1H\}$ NMR data for **2a**−**2d**. The chemical shifts and the $^1J_{PtP}$ values for two phosphorus nuclei in **2a**, **2b**, and **2d** are comparable to one another, showing nearly identical electronic properties of silyl and boryl ligands. The PEt_3 complex **2c** exhibits only one broad signal with ^{195}Pt satellites even at low temperature (−50 °C), probably due to the occurrence of rapid dissociation of PEt_3 ligands.

Insertion of Phenylacetylene into Silyl-Boryl Complexes. Complex **2a** smoothly reacted with phenylacetylene in CD_2Cl_2 at room temperature to give the insertion complex **3a**, quantitatively (Scheme 3). When an excess amount of phenylacetylene (5−10 molar quantity) was employed, the reaction was completed in 2 h. As seen from Figure 1b, the $^{31}P\{^1H\}$ NMR spectrum of **3a** exhibits two sets of doublets at δ −23.2 ($^2J_{PP}$ = 22 Hz, $^1J_{PtP}$ = 1276 Hz) and −29.5 ($^2J_{PP}$ = 22 Hz, $^1J_{PtP}$ = 1907 Hz), respectively. The former has ^{29}Si satellites,

(7) Complexes **2a**−**2d** may be prepared in benzene or toluene, while their isolation is rather difficult due to high solubility in these solvents. Preparation in THF or CH_2Cl_2 was unsuccessful owing to instability of $Pt(cod)_2$.

(8) Analytically pure **2d** could not be obtained due to contamination of impurities.

Scheme 3

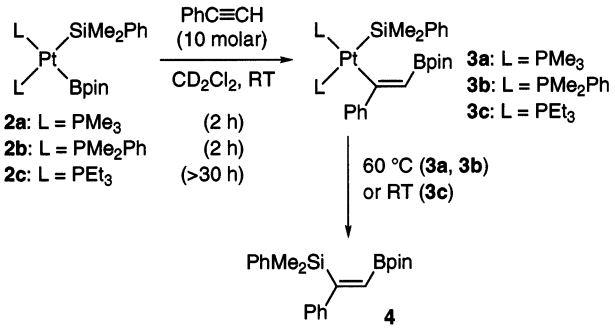

with the $^2J_{SiP}$ value (168 Hz) comparable to that of **2a** (148 Hz), showing the presence of a Pt−Si bond. On the other hand, the signal broadening observed for **2a** bearing a Pt−B bond does not occur for **3a**. Hence, the selective insertion of phenylacetylene into the Pt−B bond has been evidenced.

Complex **2b** exhibited reactivity comparable to **2a**, whereas **2d** was unreactive even at 60 °C. Complex **2c** was moderately reactive and gradually converted into the insertion complex at room temperature. In this case, the resulting **3c** subsequently underwent C−Si reductive elimination to give (*Z*)-α-silyl-*β*-borylstyrene **4** (vide infra).

In the ^{1}H NMR spectrum of **3a**, the vinylic proton signal appeared at δ 7.00 as a doublet of doublets due to the spin−spin coupling with the two phosphorus nuclei ($^4J_{PH}$ = 17.7 and 4.5 Hz, $^3J_{PtH}$ = 122.4 Hz). The ^{13}C{^{1}H} NMR spectrum exhibited two sets of signals arising from the vinylic carbons at δ 120.0 (br) and 191.9 (dd, $^2J_{PC}$ = 98 and 16 Hz). The latter at the lower magnetic field, which is assignable to the α-vinylic carbon on the basis of the chemical shift and the $^2J_{PC}$ coupling constants, disappeared in a DEPT NMR spectrum, whereas the former remained unchanged. Accordingly, the occurrence of regioselective insertion of phenylacetylene, leading to the form *cis*-Pt{C(Ph)═CH(Bpin)}(SiMe$_2$Ph)(PMe$_3$)$_2$, was clearly indicated. The characteristic NMR signals were similarly observed for **3b**.

Figure 2 shows the X-ray structure of **3b**, which is consistent with the NMR observations. The phenyl group is bonded to the α-vinylic carbon of the alkenyl ligand, and the platinum and boron atoms are situated at mutually cis positions. The C(1)−C(2) distance (1.366(9) Å) is in a typical range of C−C double bonds. The Pt−P(1) bond (2.383(2) Å) is significantly longer than the Pt−P(2) bond (2.299(2) Å), reflecting the greater trans influence of the silyl ligand than the alkenyl ligand.

Reductive Elimination from Silyl-Alkenyl Complexes. The PMe$_3$- and PMe$_2$Ph-coordinated complexes **3a** and **3b** underwent C−Si reductive elimination under heated conditions (Scheme 3). The reactions performed at 60 °C in toluene-d_8 were completed in 30 (**3a**) and 6 h (**3b**), respectively, to afford (*Z*)-α-silyl-*β*-borylstyrene **4**, the structure of which was identical with that previously prepared by catalytic reactions.[6b,d] The reductive elimination was significantly accelerated by addition of PhC≡CPh to the system. For example, in the presence of 10 molar quantity of the acetylene, the reaction of **3b** was completed in 1 h at 60 °C. On the other hand, the reductive elimination was effectively retarded by free phosphines (1 molar quantity) and took several days for completion at the same temperature. Similar behavior has been reported for *cis*-alkyl(silyl)platinum(II) complexes, whose C−Si reductive elimination involves preliminary dissociation of phosphine ligand.[9]

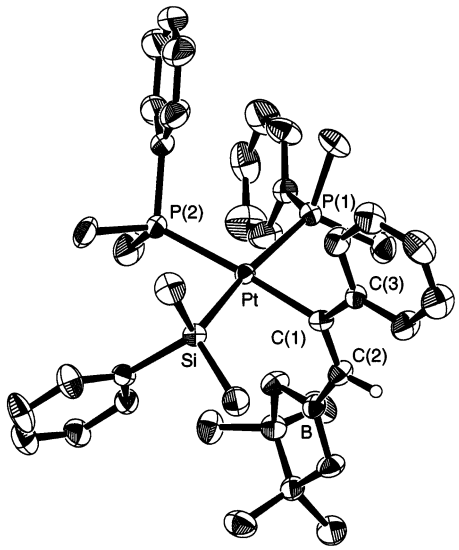

Figure 2. Molecular structure of **3b**. Thermal ellipsoids are drawn at the 30% probability level. Selected bond distances (Å) and angles (deg): Pt−C(1) = 2.062(7), C(1)−C(2) = 1.366(9), C(1)−C(3) = 1.501(9), C(2)−B = 1.54(1), Pt−Si = 2.371(2), Pt−P(1) = 2.383(2), Pt−P(2) = 2.299(2), Pt−C(1)−C(2) = 122.0(5), Pt−C(1)−C(3) = 118.8(4), C(2)−C(1)−C(3) = 119.2(6), C(1)−C(2)−B = 129.7(6), Si−Pt−C(1) = 83.9(2), P(1)−Pt−C(1) = 87.5(2), P(1)−Pt−P(2) = 95.90(6), P(2)−Pt−Si = 92.79(6).

The PEt$_3$-coordinated **3c** was much more reactive, and the C−Si reductive elimination giving **4** proceeded successively after the insertion of phenylacetylene into **2c**. Figure 3 shows the time course observed in CD_2Cl_2 at 20 °C, which adopts a typical pattern of consecutive reactions. The amount of **3c** reached a maximum after 7 h and then decreased gradually with increasing amount of **4**.

While the insertion complex **3c** is a transient species and could not be isolated, its formation was supported by NMR spectroscopy. Figure 4 illustrates a part of the ^{1}H NMR spectrum of the reaction solution of **2c** with phenylacetylene in CD_2Cl_2. The apparent triplet at δ 0.42 with ^{195}Pt satellites ($^3J_{PtH}$ = 30.4 Hz) and the singlet at δ 0.38 are assignable to SiMe groups of **2c** and **4**, respectively. On the other hand, SiMe signals of **3c** are observed as two sets of doublets with ^{195}Pt satellites at δ 0.20 ($^3J_{PtH}$ = 22.4 Hz) and 0.07 ($^3J_{PtH}$ = 23.4 Hz). The nonequivalency of two SiMe groups is attributable to the presence of a −C(Ph)═CH(Bpin) ligand with an unsymmetrical structure, which is perpendicularly coordinated to the Pt(SiMe$_2$Ph)(PEt$_3$)$_2$ moiety. This type of structure was confirmed for PMe$_2$Ph-coordinated analogue **3b** by X-ray diffraction analysis (Figure 2). In the ^{1}H NMR spectrum of **3b**, SiMe

(9) (a) Hasebe, K.; Kamite, J.; Mori, T.; Katayama, H.; Ozawa, F. *Organometallics* **2000**, *19*, 2022. (b) Ozawa, F.; Hikida, T.; Hasebe, K.; Mori, T. *Organometallics* **1998**, *17*, 1018. (c) Ozawa, F.; Hikida, T.; Hayashi, T. *J. Am. Chem. Soc.* **1994**, *116*, 2844. (d) Ozawa, F.; Kitaguchi, M.; Katayama, H. *Chem. Lett.* **1999**, 1289.

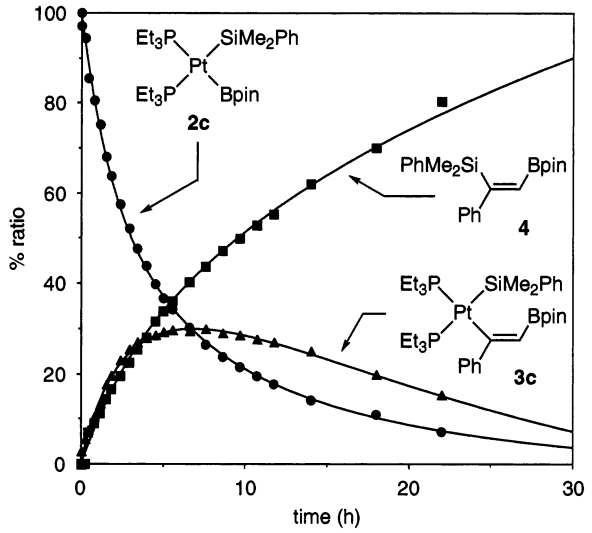

Figure 3. Time course of the reaction of **2c** with phenylacetylene (10 molar quantity) at 20 °C in CD_2Cl_2. The amount of each component at time t was determined by ^1H NMR spectroscopy.

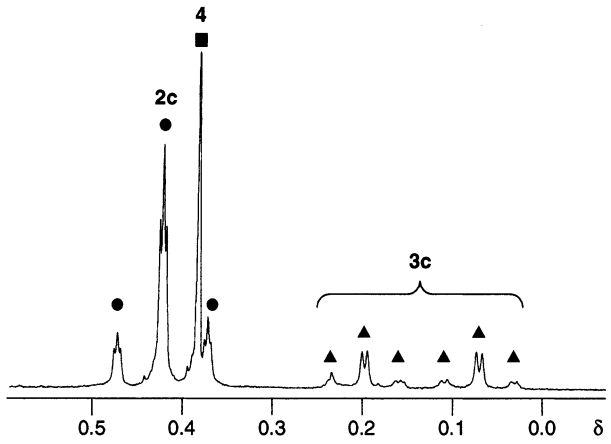

Figure 4. ^1H NMR spectrum of the reaction solution of **2c** and phenylacetylene (10 molar quantity) in CD_2Cl_2 at 20 °C. The solution consists of a 44:28:28 ratio of **2c**, **3c**, and **4**. Only the SiMe proton region is shown for clarity.

groups exhibit nonequivalent signals at δ 0.22 and 0.13, indicating restricted rotation of the −C(Ph)═CH(Bpin) ligand around the Pt−C(1) bond. Thus, when the rotation is a sufficiently slow process on an NMR time scale, the two SiMe groups may be regarded as being diastereotopic with each other to exhibit different chemical shifts. Since the rotational barrier arises mainly from steric repulsion between the −C(Ph)═CH-(Bpin) and Pt($SiMe_2Ph$)(PMe_2Ph)$_2$ moiety in **3b**, it is reasonable to assume a similar situation for **3c**, having bulkier PEt_3 ligands.

The $^{31}P\{^1H\}$ NMR signals of **3c** appeared at δ 1.4 and 3.0 as two sets of doublets ($^2J_{PP}$ = 18 Hz) with small (1251 Hz) and moderate (1965 Hz) coupling to ^{195}Pt, respectively. The $^1J_{PtP}$ values are comparable to those of **3a** and **3b** and are in appropriate magnitude for the phosphines coordinated trans to boryl and alkenyl ligands, respectively.

Kinetic Study on the Insertion of Phenylacetylene. The insertion mechanism of phenylacetylene into **2a** in CD_2Cl_2 was examined by kinetic experiments under pseudo-first-order conditions using an excess amount of phenylacetylene. Table 2 lists the rate constants (k_{obsd}) observed at various concentration of phenylacetylene and PMe_3.

Table 2. Pseudo-First-Order Rate Constants for the Insertion of Phenylacetylene into 2a[a]

run	[PhC≡CH] (M)	10^3[PMe_3] (M)	10^4k_{obsd} (s^{-1})
1	0.15	4.0	2.38(5)
2	0.25	4.0	3.8(1)
3	0.40	4.0	5.4(1)
4	0.60	4.0	6.5(3)
5	0.25	6.3	2.6(1)
6	0.25	11	1.49(3)
7	0.25	16	1.09(3)
8	0.25	25	0.71(4)

[a] In CD_2Cl_2 at 20 °C. [**2a**]$_0$ = 0.025 M.

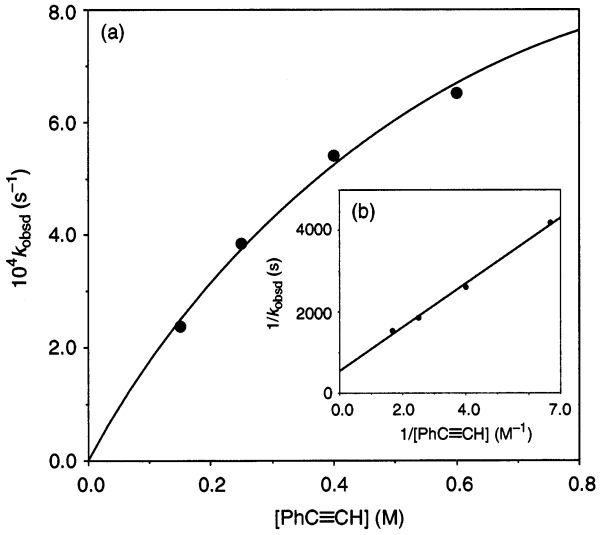

Figure 5. Effect of phenylacetylene concentration on the insertion rate of phenylacetylene into **2a** in CD_2Cl_2 in the presence of added PMe_3 at 20 °C. Initial concentration: [**2a**] = 25 mM, [PMe_3] = 4.0 mM.

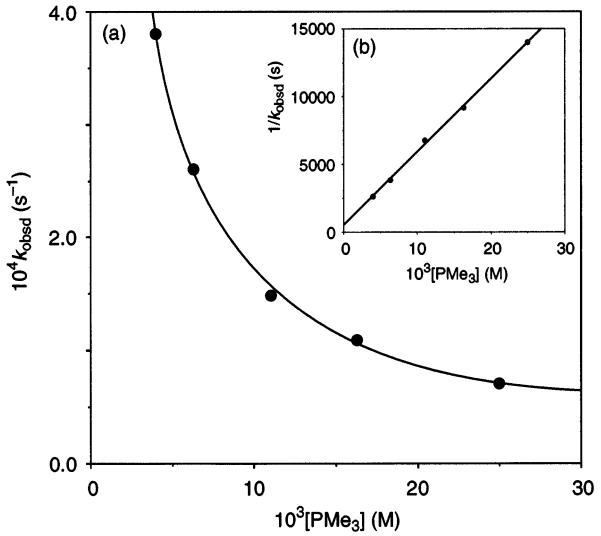

Figure 6. Effect of added PMe_3 on the insertion rate of phenylacetylene into **2a** in CD_2Cl_2 at 20 °C. Initial concentration: [**2a**] = 25 mM, [PhC≡CH] = 0.25 M.

The reaction rate increased with increase in the concentration of phenylacetylene (runs 1−4; Figure 5a). On the other hand, the reaction progress was effectively retarded by free PMe_3 (runs 2 and 5−8; Figure 6a). The reciprocals of k_{obsd} values exhibited good linear correla-

Scheme 4

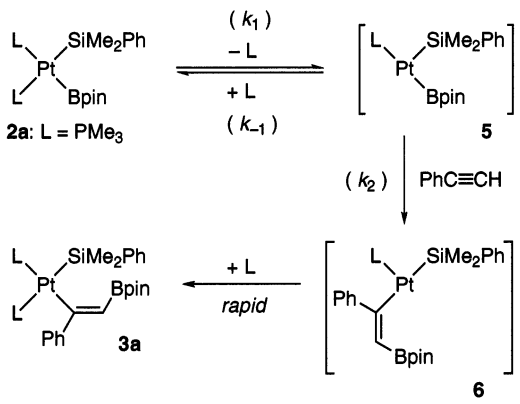

tion with 1/[PhC≡CH] and [PMe_3] values, respectively (Figures 5b and 6b).

Scheme 4 shows our proposed mechanism. The first step is dissociation of one of the PMe_3 ligands (L) from **2a**. The three-coordinate silyl-boryl intermediate **5** thus generated successively undergoes insertion of phenylacetylene into the Pt−B bond via prior coordination of phenylacetylene to the vacant site of **5**. The resulting **6** is then converted into the final product **3a** by trans to cis isomerization followed by coordination of L. This mechanism is essentially the same as that previously proposed for the acetylene insertion into *cis*-bis(silyl)- and *cis*-bis(boryl)platinum(II) complexes.[3b,4a,b]

Steady-state approximation for the concentration of **5** leads to the following equation:

$$\frac{d[\mathbf{5}]}{dt} = k_1[\mathbf{2a}] - k_{-1}[PMe_3][\mathbf{5}] - k_2[PhC{\equiv}CH][\mathbf{5}] = 0 \quad (1)$$

Thus,

$$[\mathbf{5}] = \frac{k_1[\mathbf{2a}]}{k_{-1}[PMe_3] + k_2[PhC{\equiv}CH]} \quad (2)$$

If the steady-state for **5** holds and the conversion of **6** to **3a** is sufficiently more rapid than the acetylene insertion into **5**, the rate of formation of **3a** is expressed as follows:

$$\frac{d[\mathbf{3a}]}{dt} = -\frac{d[\mathbf{2a}]}{dt} = k_2[PhC{\equiv}CH][\mathbf{5}] \quad (3)$$

Substitution of eq 2 into eq 3 yields the final rate expression:

$$-\frac{d[\mathbf{2a}]}{dt} = \frac{k_1k_2[PhC{\equiv}CH]}{k_{-1}[PMe_3] + k_2[PhC{\equiv}CH]}[\mathbf{2a}] \quad (4)$$

Accordingly, the following relation between the k_{obsd} value and the concentration of phenylacetylene and PMe_3 can be obtained:

$$\frac{1}{k_{obsd}} = \frac{k_{-1}[PMe_3]}{k_1k_2[PhC{\equiv}CH]} + \frac{1}{k_1} \quad (5)$$

Equation 5 was fully consistent with the kinetic data. Thus, the k_{-1}/k_1k_2 values, estimated from the slopes of Figures 5b and 6b, were in good agreement with each other: 1.35(6) × 10^5 and 1.36(2) × 10^5 s. Moreover, reciprocals of the intercepts in these figures, which correspond to the rate constant k_1 for the dissociation of PMe_3 from **2a**, were in agreement with each other: 1.8(4) × 10^{-3} and 2.0(5) × 10^{-3} s^{-1}.

Discussion

We have demonstrated that all the elementary processes presumed for catalytic silylborylation of phenylacetylene with $PhMe_2SiBpin$ (**1a**) can be examined stepwise by using platinum complexes. Each of the processes has been found to be significantly affected by the type of tertiary phosphine ligands employed. Thus, the oxidative addition (step a in Scheme 1) tends to proceed preferably with compact phosphines such as PMe_3 and PMe_2Ph. The subsequent insertion (step b) also proceeds more readily with these phosphine ligands (**2a** and **2b**) than with the PEt_3 ligand (**2c**). As confirmed for **2a** by kinetic experiments, the insertion rate is controlled at two stages, i.e., dissociation of L from **2** and insertion of phenylacetylene via prior coordination of the acetylene to **5** (Scheme 4). Since the former stage is easier for bulkier phosphines in a general sense, it is considered that the insertion rate is mainly dependent on the ease of the latter stage. Although we could not evaluate the coordination and insertion steps in the latter stage, separately, it seems reasonable that the bulkier phosphine inhibits the coordination of phenylacetylene to cause the slower insertion rate. On the other hand, the final process leading to C−Si reductive elimination (step c) has been found to be easier for the complex bearing bulkier phosphine ligands (i.e., **3c** ≫ **3b** > **3c**). As suggested by preliminary kinetic experiments for **3b**, this process involves prior phosphine dissociation to give the [Pt{C(Ph)═CH(Bpin)}($SiMe_2$Ph)L] intermediate, which reductively eliminates (*Z*)-α-silyl-*β*-borylstyrene **4**. Accordingly, key roles of monophosphine species in steps b and c in Scheme 1 (i.e., $n = 1$) have been evidenced.

We have also confirmed that the insertion of phenylacetylene into silyl-boryl complexes **2a**−**2c** occurs exclusively at the Pt−B bond.[10] This finding supports the previously proposed mechanism for catalytic silylborylation.[6] Since both bis(silyl)- and bis(boryl)platinum(II) complexes are known to undergo acetylene insertion under similar reaction conditions,[3b,4a−d] the perfect selection of the insertion site deserves a discussion.

There are two stages possibly responsible for the site selectivity (Scheme 5). One is the phosphine dissociation from **2**. Thus, if the dissociation of the phosphine trans to the silyl ligand is much easier than the other, phenylacetylene may selectively insert into the Pt−B bond via the intermediates **5** and **7**. However, as judging from the very close $^1J_{PtP}$ values of the two phosphine ligands observed for **2a**−**2c** (Table 1), this possibility seems unlikely. The other stage that we have to examine is the insertion of phenylacetylene into the coordinatively unsaturated species **5** and its isomer **5′**. At this stage, reflecting the bulkiness of the $SiMe_2Ph$ ligand compared with the Bpin ligand, acetylene coordination to **5** will be sterically advantageous over the

(10) For insertion of acetylene into other transition metal boryl complexes, see: Clark, G. R.; Irvine, G. J.; Roper, W. R.; Wright, L. J. *Organometallics* **1997**, *16*, 5499. Onozawa, S.-y.; Tanaka, M. *Organometallics* **2001**, *20*, 5956.

Scheme 5

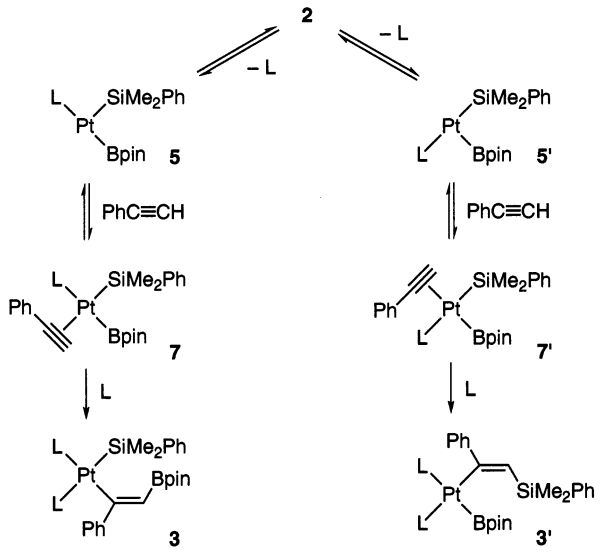

coordination to **5′**. Furthermore, on the subsequent migratory insertion step, we may expect another reason for the Bpin group migration in **7** taking place in preference to the $SiMe_2Ph$ group migration in **7′**, which is related to orbital interaction during the migration. Thus, the migration of sp^3-hybridized ligands is known to involve distortion energy, caused by direction change of the sp^3 orbital from metal to carbon.[11] For SiH_3 the distortion energy has been estimated to be 13.8 kcal/mol by theoretical calculation.[11b] On the other hand, the Bpin ligand in **7** with sp^2-hybridization may migrate more easily to the acetylenic carbon via the participation of the p_π orbital on B, which will reduce the energy growth associated with the direction change of the sp^2 orbital from metal to carbon.[12]

Apart from the kinetic viewpoints, the insertion into the Pt−B bond seems preferable in a thermodynamic sense as well. Thus, Sakaki et al. have recently provided the following bond energies (kcal mol^{-1}): Pt−$B(OH)_2$ (64.4), Pt−SiH_3 (54.2), H_3C−$B(OH)_2$ (109.7), H_3C−SiH_3 (86.0).[11c] It is seen that the difference between C−B and C−Si bonds (23.7) is significantly larger than that between Pt−B and Pt−Si bonds (10.2). While our consideration for the site selectivity is not conclusive, the present findings provide an interesting opportunity for further studies, especially for theoretical investigations.

Experimental Section

General Procedures. All manipulations were carried out under a nitrogen atmosphere using conventional Schlenk techniques. Nitrogen gas was dried by passing through P_2O_5 (Merck, SICAPENT). NMR spectra were recorded on a Varian Mercury 300 spectrometer. Chemical shifts are reported in δ (ppm) referred to an internal $SiMe_4$ standard for ^1H and ^{13}C NMR and to an external 85% H_3PO_4 standard for ^{31}P NMR. GLC analysis was performed on a Shimadzu GC-14B instrument equipped with a FID detector and a CBP-1 capillary column (25 m × 0.25 mm). Bis(1,5-cyclooctadiene)platinum(0)[13] and silylboranes (**1a**, **1b**)[14] were prepared according to literature procedures. THF, Et_2O, pentane, and toluene were dried over sodium benzophenone ketyl and distilled prior to use. CH_2Cl_2 was dried over CaH_2 and distilled prior to use. CD_2Cl_2 was dried over $LiAlH_4$, vacuum transferred, and stored under a nitrogen atmosphere.

Preparation of *cis*-Pt(SiMe$_2$Ph)(Bpin)(PMe$_3$)$_2$ (2a). To a white suspension of $Pt(cod)_2$ (226 mg, 0.55 mmol) in Et_2O (20 mL) were successively added PMe_3 (84 mg, 1.1 mmol) and $PhMe_2SiBpin$ (**1a**, 144 mg, 0.55 mmol) at 0 °C. The mixture was stirred at room temperature for 1 h to give a pale yellow homogeneous solution, which was concentrated to dryness by pumping. The resulting oily material was cooled to −78 °C and dissolved in Et_2O (1 mL). Slow addition of pentane (3 mL) with vigorous stirring at the same temperature led to precipitation of a pale yellow solid of **2a**, which was collected by filtration, washed with pentane (3 mL × 3), and dried under vacuum (175 mg, 51%).

2a. ^1H NMR (CD_2Cl_2, −50 °C): δ 0.39 (dd, $^4J_{PH}$ = 1.5 and 1.2 Hz, $^3J_{PtH}$ = 31.2 Hz, 6H, SiMe), 1.15 (d, $^2J_{PH}$ = 6.9 Hz, $^3J_{PtH}$ = 16.2 Hz, 9H, PMe), 1.26 (s, 12H, Bpin(Me)), 1.56 (d, $^2J_{PH}$ = 7.8 Hz, $^3J_{PtH}$ = 20.6 Hz, 9H, PMe), 7.08−7.23 (m, 3H, Ph), 7.50−7.60 (m, 2H, Ph). $^{13}C\{^1H\}$ NMR (CD_2Cl_2, −50 °C): δ 6.4 (t, $^3J_{PC}$ = 6 Hz, $^2J_{PtC}$ = 96 Hz, SiMe), 18.0 (m, $^1J_{PC}$ = 24 Hz, $^2J_{PtC}$ = 20 Hz, PMe), 18.6 (m, $^1J_{PC}$ = 25 Hz, $^2J_{PtC}$ = 31 Hz, PMe), 26.5 (s, Bpin(Me)), 81.2 (d, $^4J_{PC}$ = 3 Hz, $^3J_{PtC}$ = 33 Hz, Bpin), 126.3 (s, Ph), 126.7 (s, SiPh), 134.1 (s, $^3J_{PtC}$ = 23 Hz, SiPh), 152.9 (t, $^2J_{PC}$ = 7 Hz, $^2J_{PtC}$ = 29 Hz, SiPh). $^{31}P\{^1H\}$ NMR (CD_2Cl_2, −50 °C): δ −17.4 (d, $^2J_{PP}$ = 29 Hz, $^1J_{PtP}$ = 1374 Hz, $^2J_{SiP}$ = 148 Hz), −19.0 (br, $^1J_{PtP}$ = 1375 Hz). Anal. Calcd for $C_{20}H_{41}O_2BSiP_2Pt$: C, 39.41; H, 6.78. Found: C, 39.67; H, 6.68.

Complexes **2b** and **2c** were similarly prepared in 72 and 86% yield, respectively, by using PMe_2Ph and PEt_3 in place of PMe_3. The synthesis of **2d** followed essentially the same procedure as **2a**−**2c**, except for the reaction time. Thus, the reaction of $Pt(cod)_2$, PMe_3, and $PhMe_2SiBdmeda$ (**1b**) in Et_2O took 12 h for completion at room temperature. Complex **2d** was obtained as a pale yellow solid in 48% yield, which was pure by ^{31}P NMR spectroscopy but contained a small amount (ca. 3%) of organic impurities, as confirmed by ^1H NMR spectroscopy. Several attempts to obtain analytically pure **2d** by recrystallization were unsuccessful.

2b. ^1H NMR (CD_2Cl_2, −50 °C): δ 0.37 (d, $^4J_{PH}$ = 2.1 Hz, $^3J_{PtH}$ = 32.1 Hz, 6H, SiMe), 1.04 (s, 12H, Bpin(Me)), 1.07 (d, $^2J_{PH}$ = 6.9 Hz, $^3J_{PtH}$ = 17.4 Hz, 6H, PMe), 1.45 (d, $^2J_{PH}$ = 7.5 Hz, $^3J_{PtH}$ = 21.3 Hz, 6H, PMe), 7.10−7.45 (m, 13H, Ph), 7.56−7.64 (m, 2H, Ph). $^{13}C\{^1H\}$ NMR (CD_2Cl_2, −50 °C): δ 6.5 (t, $^3J_{PC}$ = 5 Hz, $^2J_{PtC}$ = 95 Hz, SiMe), 16.1 (m, $^1J_{PC}$ = 25 Hz, $^3J_{PC}$ = 5 Hz, $^2J_{PtC}$ = 24 Hz, PMe), 16.7 (m, $^1J_{PC}$ = 26 Hz, $^3J_{PC}$ = 5 Hz, $^2J_{PtC}$ = 37 Hz, PMe), 26.3 (s, Bpin(Me)), 81.2 (d, $^4J_{PC}$ = 3 Hz, $^3J_{PtC}$ = 33 Hz, Bpin), 126.5 (s, SiPh), 126.8 (s, SiPh), 127.9 (d, $^3J_{PC}$ = 6 Hz, PPh), 128.0 (d, $^3J_{PC}$ = 5 Hz, PPh), 129.2 (s, PPh), 129.3 (s, PPh), 130.7 (d, $^2J_{PC}$ = 12 Hz, PPh), 134.4 (s, $^3J_{PtC}$ = 24 Hz, SiPh), 138.6 (dd, $^1J_{PC}$ = 40 Hz, $^3J_{PC}$ = 3 Hz, PPh), 139.8 (dd, $^1J_{PC}$ = 38 Hz, $^3J_{PC}$ = 3 Hz, PPh), 152.5 (t, $^3J_{PC}$ = 6 Hz, $^2J_{PtC}$ = 35 Hz, SiPh). $^{31}P\{^1H\}$ NMR (CD_2Cl_2, −50 °C): δ −5.2 (br, $^1J_{PtP}$ = 1391 Hz), −6.4 (d, $^2J_{PP}$ = 30 Hz, $^1J_{PtP}$ = 1404 Hz, $^2J_{SiP}$ = 139 Hz). Anal. Calcd for $C_{30}H_{45}O_2BSiP_2Pt$: C, 49.12; H, 6.18. Found: C, 49.26; H, 6.06.

(11) (a) Sakaki, S.; Biswas, B.; Musashi, Y.; Sugimoto, M. *J. Organomet. Chem.* **2000**, *611*, 288. (b) Biswas, B.; Sugimoto, M.; Sakaki, S. *Organometallics* **1999**, *18*, 4015. (c) Sakaki, S.; Kai, S.; Sugimoto, M. *Organometallics* **1999**, *18*, 4825.

(12) (a) Insertion of C−C multiple bonds into a Pt−B bond of *cis*-Pt{$B(OH)_2$}$_2$(PH_3)$_2$ has been examined theoretically.[5a] Although no details of orbital interaction have been described, the transition-state structure optimized for the migratory insertion in *cis*-Pt{$B(OH)_2$}$_2$(η^2-H_2C=CH_2)(PH_3) to give Pt{$CH_2CH_2B(OH)_2$}{$B(OH)_2$}(PH_3) indicates the participation of the p_π orbital on B. Thus, judging from the geometry around the boron atom, the sp^2 orbital is clearly oriented toward one of the olefinic carbons to make a B−C bond (d(B−C) = 1.645 Å), while the boron still interacts with platinum to a considerable extent (d(Pt−B) = 2.515 Å) via the p_π orbital. (b) Importance of the paraticipation of the boron p_π orbital has been demonstrated for oxidative addition of $(HO)_2B$−XH_3 (X = C, Si, Ge, Sn) to M(PH_3)$_2$ (M = Pd, Pt).[11c]

(13) Crascall, L. E.; Spencer, J. L. *Inorg. Synth.* **1990**, *28*, 126.

(14) (a) Biffar, W.; Nöth, H.; Schwerthöffer, R. *Liebigs Ann. Chem.* **1981**, 2067. (b) Buynak, J. D.; Geng, B. *Organometallics* **1995**, *14*, 3112. (c) Suginome, M.; Matsuda, T.; Ito, Y. *Organometallics* **2000**, *19*, 4647.

2c. ^{1}H NMR (CD_2Cl_2, −50 °C): δ 0.32 (s, $^3J_{PtH}$ = 30.8 Hz, 6H, SiMe), 0.77 (dt, $^3J_{PH}$ = 15.3 Hz, $^3J_{HH}$ = 7.5 Hz, 9H, PCH_2CH_3), 1.00 (dt, $^3J_{PH}$ = 15.6 Hz, $^3J_{HH}$ = 7.5 Hz, 9H, PCH_2CH_3), 1.22 (s, 12H, Bpin(Me)), 1.35 (m, 6H, PCH_2CH_3), 1.89 (m, 6H, PCH_2CH_3), 7.04−7.18 (m, 3H, Ph), 7.45 (d, $^3J_{HH}$ = 6.6 Hz, 2H, Ph). ^{13}C{^{1}H} NMR (CD_2Cl_2, −50 °C): δ 6.7 (t, $^3J_{PC}$ = 10 and 4 Hz, $^2J_{PtC}$ = 97 Hz, SiMe), 8.36 (s, $^3J_{PtC}$ = 16 Hz, PCH_2CH_3), 8.43 (s, $^3J_{PtC}$ = 16 Hz, PCH_2CH_3), 17.4 (m,[15] $^1J_{PC}$ = 26 Hz, PCH_2CH_3), 17.9 (m,[15] $^1J_{PC}$ = 26 Hz, PCH_2CH_3), 26.6 (s, Bpin(Me)), 81.2 (s, $^3J_{PtC}$ = 33 Hz, Bpin), 125.9 (s, SiPh), 126.4 (s, SiPh), 133.8 (s, $^3J_{PtC}$ = 18 Hz, SiPh), 153.0 (t, $^3J_{PC}$ = 7 Hz, $^2J_{PtC}$ = 30 Hz, SiPh). ^{31}P{^{1}H} NMR (CD_2Cl_2, −50 °C): δ 14.8 (br, $^1J_{PtP}$ = 1468 Hz). Anal. Calcd for $C_{26}H_{53}O_2BSiP_2Pt$: C, 45.02; H, 7.70. Found: C, 44.49; H, 7.80.

2d. ^{1}H NMR (CD_2Cl_2, −50 °C): δ 0.16 (d, $^4J_{PH}$ = 2.4 Hz, $^3J_{PtH}$ = 30.6 Hz, 6H, SiMe), 1.08 (d, $^2J_{PH}$ = 6.6 Hz, $^3J_{PtH}$ = 15.6 Hz, 9 H, PMe), 1.38 (d, $^2J_{PH}$ = 7.8 Hz, $^3J_{PtH}$ = 21.0 Hz, 9 H, PMe), 2.62 (s, 6H, NMe), 3.01 (s, 4H, NCH_2), 7.06−7.20 (m, 3H, Ph), 7.48−7.56 (m, 2H, Ph). ^{13}C{^{1}H} NMR (CD_2Cl_2, −50 °C): δ 3.6 (t, $^3J_{PC}$ = 11 and 5 Hz, $^2J_{PtC}$ = 96 Hz, SiMe), 15.9 (dd, $^1J_{PC}$ = 22 Hz, $^3J_{PC}$ = 5 Hz, $^2J_{PtC}$ = 19 Hz, PMe), 16.3 (dd, $^1J_{PC}$ = 25 Hz, $^3J_{PC}$ = 5 Hz, $^2J_{Pt-C}$ = 32 Hz, PMe), 25.2 (s, N(Me)*C*), 34.2 (s, $^3J_{PtC}$ = 37 Hz, NMe), 123.5 (s, SiPh), 124.2 (s, SiPh), 131.8 (s, $^3J_{PtC}$ = 22 Hz, SiPh), 151.6 (dd, $^3J_{PC}$ = 7 and 5 Hz, SiPh). ^{31}P{^{1}H} NMR (CD_2Cl_2, −50 °C): δ −12.6 (d, $^2J_{PP}$ = 24 Hz, $^1J_{PtP}$ = 1465 Hz, $^2J_{SiP}$ = 159 Hz), −14.8 (br, $^1J_{PtP}$ = 1349 Hz).

Attempt at Preparation of *cis*-Pt(SiMe$_2$Ph)(Bpin)-(PMePh$_2$)$_2$. A mixture of Pt(cod)$_2$ (119 mg, 0.29 mmol), $PMePh_2$ (116 mg, 0.58 mmol), and $PhMe_2SiBPin$ (76 mg, 0.29 mmol) in Et_2O (10 mL) was stirred at room temperature for 1 h. The initially white suspension gradually turned into a reddish orange solution, whose ^{31}P{^{1}H} NMR spectrum exhibited only a singlet signal at δ 11.8 with ^{195}Pt satellites ($^1J_{PtP}$ = 1460 Hz). The solution was concentrated to dryness by pumping to give an orange oily material, which was cooled to −78 °C and treated with a small amount of Et_2O (ca. 1 mL) to afford an orange precipitate. The supernatant was removed by filtration, and the precipitate was washed with pentane (2 mL × 3) and dried under vacuum (142 mg). The ^{31}P{^{1}H} NMR spectrum measured in CD_2Cl_2 exhibited a number of unidentified peaks, together with the signal assignable to the silyl-boryl complex (ca. 50%). The formation of a silyl-boryl complex was strongly suggested by the appearance of a SiMe signal at δ 0.19 in the ^{1}H NMR spectrum, which had ^{195}Pt satellites with the $^3J_{PtP}$ value (30.0 Hz) comparable to that of **2a**−**2c**.

Preparation of *cis*-Pt{C(Ph)═CH(Bpin)}(SiMe$_2$Ph)-(PMe$_3$)$_2$ (3a). To a solution of **2a** (155 mg, 0.25 mmol) in toluene (10 mL) was added phenylacetylene (127 mg, 1.24 mmol) at room temperature. The starting **2a** disappeared in 2 h, as confirmed by ^{31}P NMR spectroscopy, to be replaced by a single product assignable to the title compound **3a**. Solvent was removed by pumping, and the pale yellow residue was dried overnight under vacuum at room temperature. This product was cooled to −78 °C, dissolved in a minimum amount of Et_2O (ca. 0.5 mL), and then treated with pentane (2 mL) with vigorous stirring to afford a white precipitate of **3a**, which was collected by filtration, washed with pentane (2 mL × 2) at −78 °C, and dried under vacuum at room temperature (96 mg, 53%). The insertion complex **3b** was similarly obtained in 58% yield.

3a. ^{1}H NMR (CD_2Cl_2, 20 °C): δ −0.03 (d, $^4J_{PH}$ = 2.1 Hz, $^3J_{PtH}$ = 24.9 Hz, 3H, SiMe), 0.13 (d, $^4J_{PH}$ = 2.1 Hz, $^3J_{PtH}$ = 23.7 Hz, 3H, SiMe), 1.24 (d, $^2J_{PH}$ = 9.0 Hz, $^3J_{PtH}$ = 18.6 Hz, 9H, PMe), 1.26 (s, 6H, Bpin(Me)), 1.29 (d, $^2J_{PH}$ = 8.4 Hz, $^3J_{PtH}$ = 16.2 Hz, 9H, PMe), 1.30 (s, 6H, Bpin(Me)), 7.00 (dd, $^4J_{PH}$ = 17.7 and 4.5 Hz, $^3J_{PtH}$ = 122.4 Hz, 1H, PtC═CH), 7.0−7.9 (m, 10H, Ph). ^{13}C{^{1}H} NMR (CD_2Cl_2, 20 °C): δ 4.9 (dd, $^3J_{PC}$ = 6 and 2 Hz, $^2J_{PtC}$ = 70 Hz, SiMe), 5.5 (dd, $^3J_{PtC}$ = 6 and 3 Hz, $^2J_{PtC}$ = 70 Hz, SiMe), 16.7 (dd, $^1J_{PC}$ = 24 Hz, $^3J_{PC}$ = 2 Hz, $^2J_{PtC}$ = 21 Hz, PMe), 19.0 (dd, $^1J_{PC}$ = 29 Hz, $^3J_{PC}$ = 5 Hz, $^2J_{PtC}$ = 29 Hz, PMe), 25.2 (s, Bpin(Me)), 25.7 (s, Bpin(Me)), 82.2 (s, Bpin), 120.0 (br, PtC = *C*H), 126.5 (s, Ph), 126.7 (s, Ph), 127.0 (s, Ph), 127.4 (s, Ph), 129.4 (d, $^4J_{PC}$ = 2 Hz, $^3J_{PtC}$ = 48 Hz, Ph), 135.0 (d, $^4J_{PC}$ = 2 Hz, $^3J_{PtC}$ = 23 Hz, SiPh), 152.3 (dd, $^3J_{PC}$ = 8 and 4 Hz, SiPh), 152.9 (d, $^2J_{PC}$ = 5 Hz, PtC(*Ph*)═C), 191.9 (dd, $^2J_{PC}$ = 98 and 16 Hz, Pt*C* = CH). ^{31}P{^{1}H} NMR (CD_2Cl_2, 20 °C): δ −23.2 (d, $^2J_{PP}$ = 22 Hz, $^1J_{PtP}$ = 1276 Hz, $^2J_{SiP}$ = 168 Hz), −29.5 (d, $^2J_{PP}$ = 22 Hz, $^1J_{PtP}$ = 1907 Hz). Anal. Calcd for $C_{28}H_{47}O_2BSiP_2Pt$: C, 47.26; H, 6.66. Found: C, 46.86; H, 6.87.

3b. ^{1}H NMR (CD_2Cl_2, 20 °C): δ 0.13 (d, $^4J_{PH}$ = 2.4 Hz, $^3J_{PtH}$ = 24.6 Hz, 3H, SiMe), 0.22 (d, $^4J_{PH}$ = 1.8 Hz, $^3J_{PtH}$ = 24.6 H, 3H, SiMe), 1.01 (d, $^2J_{PH}$ = 8.4 Hz, $^3J_{PtH}$ = 22.8 Hz, 3H, PMe), 1.04 (d, $^2J_{PH}$ = 8.1 Hz, $^3J_{PtH}$ = 22.8 Hz, 3H, PMe), 1.05 (d, $^2J_{PH}$ = 7.8 Hz, $^3J_{PtH}$ = 15.6 Hz, 3H, PMe), 1.26 (d, $^2J_{PH}$ = 8.1 Hz, $^3J_{PtH}$ = 16.2 Hz, 3H, PMe), 1.38 (s, 6H, Bpin(Me)), 1.41 (s, 6H, Bpin(Me)), 6.92 (dd, $^4J_{PH}$ = 17.8 and 4.9 Hz, 1H, PtC═CH), 7.10−7.43 (m, 16H, Ph), 7.70 (dd, 2H, Ph), 7.96 (m, 2H, Ph). ^{13}C{^{1}H} NMR (CD_2Cl_2, 20 °C): δ 5.1 (dd, $^3J_{PC}$ = 6 and 2 Hz, $^2J_{PtC}$ = 70 Hz, SiMe), 5.9 (dd, $^3J_{PC}$ = 5 and 3 Hz, $^2J_{PtC}$ = 63 Hz, SiMe), 13.7 (dd, $^1J_{PC}$ = 25 Hz, $^3J_{PC}$ = 2 Hz, $^2J_{PtC}$ = 24 Hz, PMe), 14.4 (dd, $^1J_{PC}$ = 25 Hz, $^3J_{PC}$ = 2 Hz, $^2J_{PtC}$ = 23 Hz, PMe), 16.6 (dd, $^1J_{PC}$ = 30 Hz, $^3J_{PC}$ = 5 Hz, $^2J_{PtC}$ = 36 Hz, PMe), 17.2 (dd, $^1J_{PC}$ = 30 Hz, $^3J_{PC}$ = 5 Hz, $^2J_{PtC}$ = 31 Hz, PMe), 25.2 (s, Bpin(Me)), 25.7 (s, Bpin(Me)), 82.6 (s, Bpin), 120.6 (br, PtC = *C*H), 126.6 (s, Ph), 126.8 (s, Ph), 127.0 (s, Ph), 127.5 (s, Ph), 128.2 (d, $^3J_{PC}$ = 4 Hz, PPh), 128.3 (d, $^3J_{PC}$ = 4 Hz, PPh), 129.3 (s, Ph), 129.6 (d, $^4J_{PC}$ = 2 Hz, PPh), 129.7 (d, $^4J_{PC}$ = 2 Hz, PPh), 131.1 (d, $^2J_{PC}$ = 11 Hz, $^3J_{PtC}$ = 9 Hz, PPh), 131.3 (d, $^2J_{PC}$ = 12 Hz, $^3J_{PtC}$ = 16 Hz, PPh), 135.1 (d, $^4J_{PC}$ = 2 Hz, $^3J_{PtC}$ = 22 Hz, SiPh), 138.8 (d, $^1J_{PC}$ = 32 Hz, PPh), 139.4 (dd, $^1J_{PC}$ = 42 Hz, $^3J_{PC}$ = 5 Hz, PPh), 151.8 (dd, $^3J_{PC}$ = 9 and 5 Hz, $^2J_{PtC}$ = 59 Hz, SiPh), 152.6 (d, $^3J_{PC}$ = 5 Hz, $^2J_{PtC}$ = 30 Hz, PtC(*Ph*)═C), 191.9 (dd, $^2J_{PC}$ = 97 and 15 Hz, $^1J_{PtC}$ = 783 Hz, Pt*C*═CH). ^{31}P{^{1}H} NMR (CD_2Cl_2, 20 °C): δ −12.3 (d, $^2J_{PP}$ = 22 Hz, $^1J_{PtP}$ = 1255 Hz, $^2J_{SiP}$ = 168 Hz), −15.3 (d, $^2J_{PP}$ = 22 Hz, $^1J_{PtP}$ = 1957 Hz). Anal. Calcd for $C_{38}H_{51}O_2SiBP_2Pt$: C, 54.61; H, 6.15. Found: C, 54.19; H, 6.11.

X-ray Structural Analysis of 3b. A colorless prism having approximate dimensions of 0.13 × 0.15 × 0.40 mm, which was grown from an Et_2O solution at −70 °C, was mounted on a glass fiber. All measurements were made on a Rigaku RAXIS-RAPID imaging plate diffractometer with graphite monochromated Mo Kα radiation (λ = 0.71069 Å). Indexing was performed from two oscillations which were exposed for 1.7 min. On the basis of the unit cell dimensions, statistical analysis of intensity distribution, and successful solution and refinement of the structure, the space group was determined to be $P\bar{1}$(#2). The data were collected at 23 ± 1 °C to a maximum 2θ value of 55.0°. A total of 38 images, corresponding to 238.0° oscillation angles, were collected with two different goniometer settings. Exposure time was 0.70 min per degree. The camera radius was 127.40 mm. Readout was performed in the 0.150 mm pixel mode. Of the 19 878 reflections collected, 8779 were unique (R_{int} = 0.059); equivalent reflections were merged. The data were corrected for Lorentz and polarization effects and absorption (NUMABS). All calculations were performed with the TEXSAN Crystal Structure Analysis Package provided by Rigaku Corp. The structure was solved by heavy atom Patterson methods (PATTY) and expanded using Fourier techniques (DIRDIF94). All non-hydrogen atoms were refined anisotropically. In the final cycles of refinement, hydrogen atoms were located at idealized positions (d(C−H) = 0.95 Å) with isotropic temperature factors (B_{iso} = 1.20$B_{bonded\ atom}$) and were included in calculation without

(15) Because the two phosphorus nuclei have eventually the same chemical shift and the $^2J_{PP}$ value for the *cis*-PtP_2 moiety is moderate (ca. 30 Hz as judging from the data for **2a** and **2b**), the PCH_2 carbon signal appears as a "filled-in doublet", which has a shape intermediate between a doublet and a virtual triplet. See: Crabtree, R. H. *The Organometallic Chemistry of the Transition Metals*, 3rd ed.; Wiley: New York, 2001; pp 260−262.

Table 3. Crystal Data and Details of the Structure Determination for 3b

formula	$C_{38}H_{51}O_2SiBP_2Pt$
fw	835.75
cryst syst	triclinic
no. of reflns used for unit cell determination (2θ range, deg)	9356 (3.9−54.9)
a (Å)	10.703(1)
b (Å)	11.7187(9)
c (Å)	17.373(1)
α (deg)	101.326(3)
β (deg)	94.811(2)
γ (deg)	113.097(6)
V (Å^3)	1933.8(3)
space group	$P\bar{1}$(#2)
Z	2
D_{calcd} (g cm^{-3})	1.435
μ(Mo Kα) (cm^{-1})	37.57
2θ max (deg)	55.0
no. of reflns collected	19 878
no. of unique reflns	8779 ($R_{int} = 0.059$)
transmn factors	0.3986−0.7421
no. of obsd reflns	7551 ($I \geq 3.0\sigma(I)$)
no. of variables	406
R indices ($I \geq 2\sigma(I)$)[a]	$R_1 = 0.046$
	$R = 0.085$
	$R_w = 0.138$
	GOF = 1.27
max. Δ/σ in final cycle	0.000
max. and min. peak (e Å^{-3})	1.56, −2.07

[a] Function minimized $= \sum w(F_o^2 - F_c^2)^2$; $w = (1/[\sigma^2(F_o^2)])$. $R_1 = \sum||F_o| - |F_c||/\sum|F_o|$. $R = \sum(F_o^2 - F_c^2)/\Sigma(F_o^2)$. $R_w = [\sum w(F_o^2 - F_c^2)^2/\sum w(F_o^2)^2]^{1/2}$. GOF $= [\sum w(|F_o| - |F_c|)^2/(N_o - N_v)]^{1/2}$, where N_o and N_v stand for the number of observations and variables, respectively.

refinement of their parameters. The function minimized in least-squares was $\sum w(F_o^2 - F_c^2)^2$ ($w = 1/[\sigma^2(F_o^2)]$). Crystal data and details of data collection and refinement are summarized in Table 3. Additional information is available as Supporting Information.

Reaction of *cis*-Pt(SiMe$_2$Ph)(Bpin)(PEt$_3$)$_2$ (2c) with Phenylacetylene (Figure 3). Complex **2c** (10.4 mg, 0.015 mmol) was placed in an NMR sample tube equipped with a rubber septum cap, and the system was replaced with nitrogen gas at room temperature. Phenylacetylene (15.3 mg, 0.15 mmol) was added, and then CD_2Cl_2 was added at 0 °C so that total volume of the solution becomes 0.6 mL. The sample was placed in an NMR sample probe controlled at 20.0 ± 0.1 °C and examined by ^{1}H NMR spectroscopy. The time course of the sequence of insertion and reductive elimination processes was followed by measuring relative peak integration of the SiMe signals of **2c** (δ 0.42), *cis*-Pt{C(Ph)═CH(Bpin)}(SiMe$_2$Ph)(PEt$_3$)$_2$ (**3c**, δ 0.20 and 0.07), and (*Z*)-(PhMe$_2$Si)CPh═CH(Bpin) (**4**, δ 0.38) (see Figure 4). Compound **4** was identified using an authentic sample prepared independently by palladium-catalyzed silylborylation.[6d]

3c. ^{1}H NMR (CD_2Cl_2, 20 °C): δ 0.07 (d, $^4J_{PH} = 2.1$ Hz, $^3J_{PtH} = 23.4$ Hz, 3H, SiMe), 0.20 (d, $^4J_{PH} = 1.8$ Hz, $^3J_{PtH} = 22.4$ Hz, 3H, SiMe), 1.25 (s, 6H, Bpin(Me)), 1.26 (s, 6H, Bpin(Me)), 6.9−8.0 (m, 5H, Ph). ^{31}P{^{1}H} NMR (CD_2Cl_2, 20 °C): δ 1.4 (d, $^2J_{PP} = 18$ Hz, $^1J_{PtP} = 1251$ Hz), 3.0 (d, $^2J_{PP} = 18$ Hz, $^1J_{PtP} = 1965$ Hz). The other ^{1}H NMR signals were obscured due to overlap with the signals of **2c** and **4**.

4. ^{1}H NMR (CD_2Cl_2, 20 °C): δ 0.38 (s, 6H, SiMe), 1.09 (s, 12H, Bpin(Me)), 6.26 (s, 1H, ═CH), 6.9−7.7 (m, 10H, Ph). ^{1}H NMR (toluene-d_8, 20 °C): δ 0.50 (s, 6H, SiMe), 0.91 (s, 12H, Bpin(Me)), 6.61 (s, 1H, ═CH), 7.7−7.0 (m, 10H, Ph).

Reductive Elimination from *cis*-Pt{C(Ph)═CH(Bpin)}(SiMe$_2$Ph)−(PMe$_2$Ph)$_2$ (3b). Complex **3b** (12.5 mg, 0.015 mmol) was placed in an NMR sample tube equipped with a rubber septum cap, and the system was replaced with nitrogen gas at room temperature. Toluene-d_8 (0.6 mL) was added, and the sample was placed in an NMR sample probe controlled at 60.0 ± 0.1 °C. The reaction progress was followed by observing the relative peak intensity of the SiMe proton signals of **3b** (δ 0.59 and 0.65) and **4** (δ 0.50).

Kinetic Study of the Insertion of Phenylacetylene into 2a. The experimental procedure for the reaction of **2a** and phenylacetylene was followed. The amounts of **2a** and **3a** at time *t* were determined on the basis of relative peak integration of the SiMe proton signals of these complexes: **2a** (δ 0.39), **3a** (δ −0.03 and 0.13).

Acknowledgment. This work was supported by a Grant-in-Aid for Scientific Research from the Ministry of Education, Culture, Sports, Science and Technology, Japan.

Supporting Information Available: Details of the structure determination of **3b**, including a figure giving the atomic numbering scheme and tables of atomic coordinates, thermal parameters, and full bond distances and angles. This material is available free of charge via the Internet at http://pubs.acs.org.

OM020686Z